Engineering and Technology Journal
Journal homepage: engtechjournal.org

Effect of Tin Addition on Shape Memory Effect and Mechanical Properties of Cu-Al-Ni Shape Memory Alloy

Raad S. Ahmed Adnan [a]

[a] Materials Engineering Department, University of Technology, Baghdad, Iraq, 130013@uotechnology.edu.iq

*Corresponding author.

Submitted: 05/07/2019 Accepted: 12/10/2019 Published: 25/08/2020

K E Y W O R D S

Tin, Mechanical properties, Shape memory alloys, Shape memory effect.

A B S T R A C T

This study examines the effect of Sn additions on Cu-14%Al-4.5%Ni shape memory alloy. Sn was added in three different percentages (0.3,1,3) %. The alloys were mechanically tested both in compression test and micro hardness test. Also, a thermo-mechanical test was performed on the alloys. Results showed an increase in the transformation temperature outside the domain and also a better recovery strain with the increase of Sn percentage of 3% Sn addition showed the best results in mechanical properties while the 3% Sn showed a better Shape Memory Properties near to super elastic.

How to cite this article: R. S. Ahmed Adnan, "Effect of Sn Addition on Shape Memory Effect and Mechanical Properties of Cu-Al-Ni Shape Memory Alloy," Engineering and Technology Journal, Vol. 38, Part A, No. 08, pp. 1178-1186, 2020.
DOI: https://doi.org/10.30684/etj.v38i8A.440

1. Introduction

Since the commencement of the current century, Shape Memory Alloys (SMAs) were considered from the smart materials, their application vary from the medical uses to the military ones, and the Cu-based SMAs are widely in demand for cost effectiveness with good mechanical and shape memory properties. Cu-based alloys are a proper substitute for the (Ni-Ti) alloys in the industrial applications, like valves, actuators, Micro –Electro –Mechanical Systems (MEMSs), and damping uses, owing to their low cost, easy production as well as high range of temperature [1]. They have a good recovery strain (2-4%) and a wide range in transformation temperatures (100-170)°C [2], making them a good alternative for NiTi alloys, but their brittleness, low strength, high elastic anisotropy, and high size of grain impedes their practical use [3]. Also, their brittleness makes a difficulty to machine them but this problem can be overcome by using the electric discharge machining (EDM) process or wire electric discharge machining (WEDM) cutting process, since the fourth and the fifth element addition to any alloy can make changes in this alloy and properties [4]. So, many researches are done by adding elements to change the mechanical characteristics or to obtain a small size of grain, and shape memory characteristics to be High Temperature Shape Memory Alloys (HTSMA) [5]. The effect of modifying SMA was studied in the investigations of

Saud et al. and Abbass et al. These authors investigated the influence of the addition of fourth and fifth element to the SMAs by adding various alloying elements, such as Ti, B, Ge, and Te [6-9] Also, Ahmed Adnan et al. [10] investigated the effect of Tin addition upon the thermal properties and transformation temperature. Lopez et al. [11] investigated the influence of (Sn) particles on the (Cu-Al-Ni) SMAs. This paper aims to study the effects of Tin addition by adding three different percentages of Sn and studying the effect on the mechanical properties and the shape memory properties of Cu-Al-Ni Shape Memory Alloy.

2. Experimental Work

I. Melting

Pure Copper wires having (99.99%) purity, Aluminum foils having (99.99%) purity, and Ni powder having (99.99%) purity with a particles size range of (0.294-1.7μ) were melted in a (SiC) crucible placed in a controlled induction furnace using a controlled Argon (Ar) atmosphere at a temperature of 1200^0C, and the resulted melt was then placed in a steel die having a cylindrical shape and with a diameter of 1.4 cm. Then, the prepared ingot was first re-melted, and the pure Sn (99.99%) particles were added to the resulted melt, which was then stirred mechanically via a stirrer for 5 min in each of the three percentages (0.3%, 1.0% and 3.0% Sn) at 1100^0C. A process of homogenization was conducted for all the prepared ingots at temperature (900^0C) for a period of (30) min, and these ingots were then quenched in a brine solution containing ice. Chemical composition analysis was done by using instrument type Alloy Analyzer 3000, as shown in Table 1. A wire cutting machine was utilized for cutting these ingots into (2) groups of specimens; the first one has 2.8 cm height and 1.4 cm diameter for the (ASTM E-9) compression test, and the other one has 0.5 cm height used for the optical microscopy, scanning electron microscopy (SEM), micro hardness (HV), differential scanning calorimetry (DSC) and X-ray diffraction (XRD). These groups were categorized into three specimens' symbols of S1, S2, and S3 containing 0.3, 1.0, and 3.0% Sn, respectively in addition to the base shape memory alloy (Cu-14%Al- 4.5%Ni).

Table 1: Chemical analyses of the base (SMA) and prepared ingots.

Alloy	Cu%	Al%	Ni%	Sn%
Base	Re	14	4.5	0
S1	Re	14	4.5	0.3
S2	Re	14	4.5	1
S3	Re	14	4.5	3

II.XRD and Microstructure

The X-ray diffraction test was conducted utilizing (Shmidzoo 3000 XRD-EDX) apparatus with a copper target (Cu (α)), and (λ = 1.45 A^0). And, for microstructural test, specimens were first prepared, and then ground, polished, and finally etched into a solution that contains (HCl+ FeCl2.6H2O+methnol). Then, this test was carried out for (4) minutes of soaking time and the microstructural observations were done for the all specimens using (Kruss Optical Microscopy) and (TESCAN Easy Probe SEM).

III. DSC

In Differential Scanning Calorimetry (DSC), SETRAM DSC device model Labsys 300, a very small specimen that placed in a small crucible having a weight of (100 mg) to study the SME utilizing using a ($10^oC.min^{-1}$) heating rate and in the range of ($25\text{-}250^0$C) in the two directions endothermic and exothermic, and the results were sent to the Microsoft EXCEL program for calculating the equilibrium temperature by Eq. (1) [10].

$$T^\circ = \frac{Ms + Af}{2} \qquad (1)$$

Where,

M_s: is the starting temperature of the martensite transformation, ^{0}C

A_f: is the end temperature of the austenite transformation, ^{0}C

IV. Mechanical Properties and SME

Vickers hardness was conducted via getting five measurements and the average magnitude was used in the Vickers hardness equation. In the compression test, an apparatus (Model Larray 600) was employed to apply the loads of compression upon the alloy. A compression test was performed utilizing the testing machine (Instron 1116) to obtain the relation between the stress and strain depending on the resulted stress-strain curve. Thermo-mechanical tests were carried out by using instrument model (Larray 1200) by applying a load up to 30 KN (195 MPa) and then unloading to record the strain%. The results were used to plot the stress-strain thermo-mechanical to calculate the modulus of elasticity and the recovery strain% for austenite and martensite as Lagodus suggested by taking the slope in two directions [2, 8].

3. Results and Discussion

I. X-ray Diffraction Results

The X-ray diffraction outcomes are depicted in Figures 1, 2, 3 and 4 for the base SMA alloy and the prepared specimens, respectively. Figure 1 reveals the analysis of (XRD) for base alloy (Cu-14%Al-4.5%Ni). It is noted that the phases development exhibits the presence of the two martensitic phases γ` ($AlCu_3$) and β` ($Al_7Cu_{23}Ni$). Whereas, in Figure 2, the (XRD) analysis of the S1 shape memory alloy (Cu-14%Al-4.5%Ni-0.3%Sn) manifested the existence of pure particles of Tin together with the above mentioned two phases. Also a similar state was found into the S2 as well as S3 SMA specimens as illustrated in Figures 3 and 4, respectively.

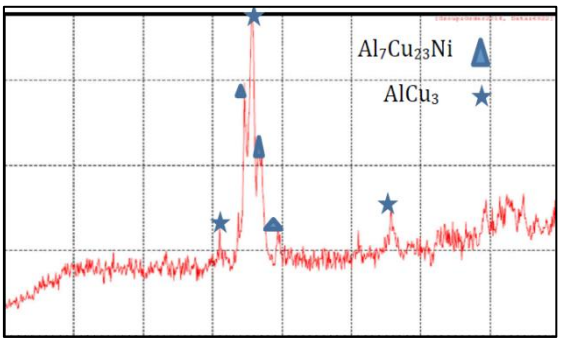

Figure 1: The results of (XRD) for the base shape memory alloy.

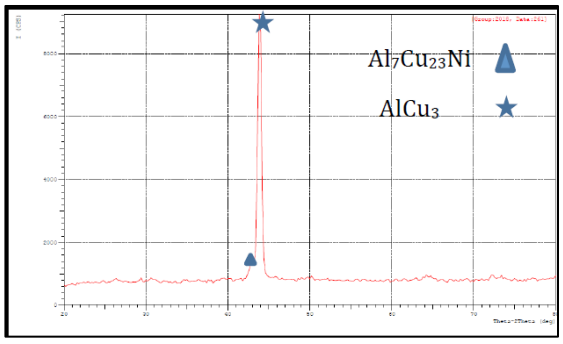

Figure 2: The results of (XRD) for the S1 shape memory alloy.

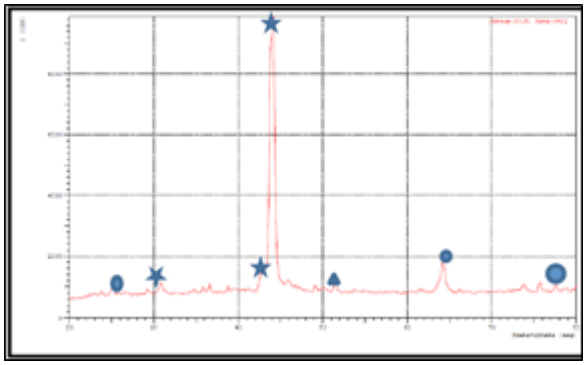

Figure 3: The results of (XRD) for the S2 shape memory alloy.

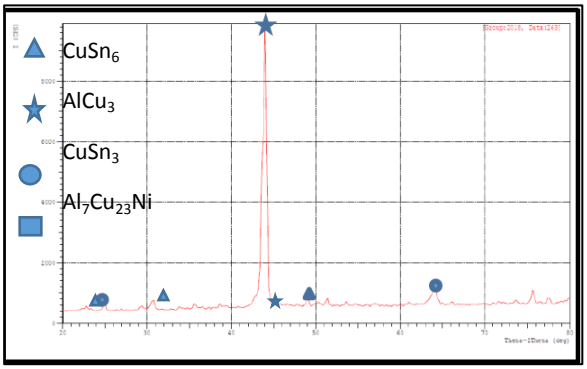

Figure 4: The results of (XRD) for the S3 shape memory alloy.

II. Microstructure

The resulted microstructures are elucidated in Figures 5, 6, 7 and 8 showing the (SEM) of the base SMA and the prepared specimens, respectively. The martensitic (β`) phase intensively existed as shown in the Figure 5 and Figure 6 in a fine-needle form, and (γ`) phase closely stacked with the martensitic (β`) phase being the main phase and (γ`) phase as Saud et al. obtained the same thing for the group of (SMA) alloys [8] and as Abbas *et al*. made after the addition of Ge [7]. Regarding such figures, Tin particles are spread in a random way as Abbass et al. inferred for the Te addition to the shape memory alloy's microstructure [6], the particles of (Sn) were randomly spread in the grain of martensite matrix in the figure (6) and with the rise of Tin percentage. Concerning Figures 7 and 8, the (β) phase is re-strained due to the spread of the (Sn) grains; particularly the martensite with a smaller size in a way same as Saud et al. [8] inferred for the (β) particles utilization and re-strained martensite phases. The outcomes of (EDS) are depicted in Figure 9 and the alloys chemical compositions.

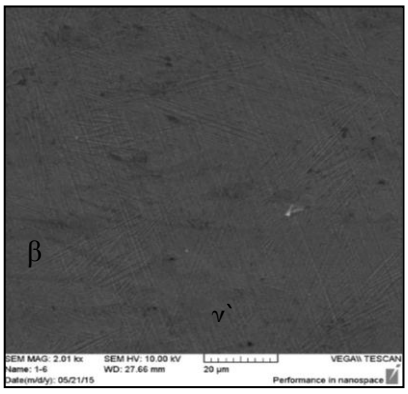

Figure 5: The base (SMA) microstructure

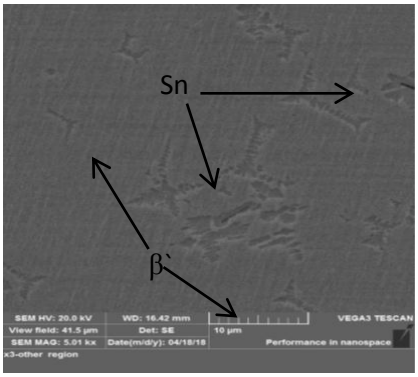

Figure 6: The (S1) alloy microstructure

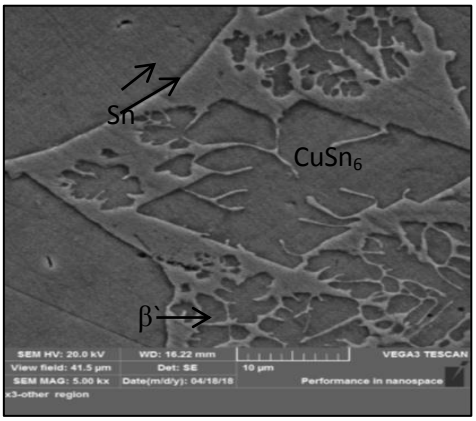

Figure 7: The (S2) alloy microstructure.

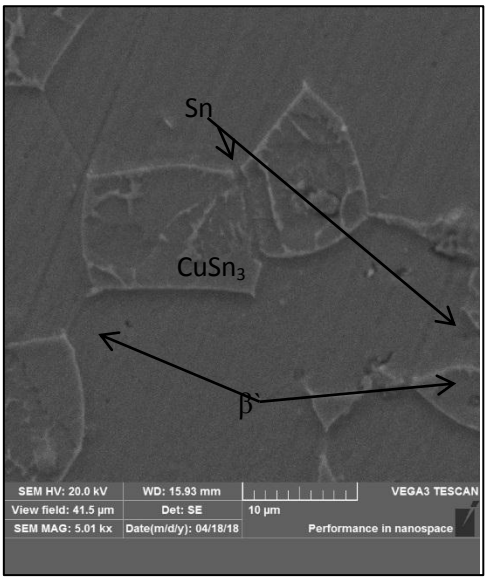

Figure 8: The (S3) alloy microstructure.

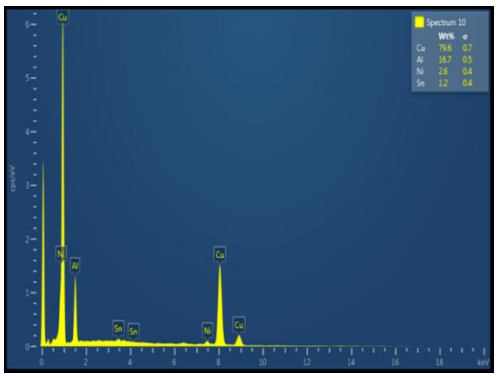

Figure 9 EDS results for S1 alloy.

III. DSC Results

Figures 10, 11, 12 and 13 reveal Thermogram of the base alloy (SMA) with the prepared specimens whereas Table 2 lists their characteristics, transformation temperatures (A_s, A_f, M_s and M_f), temperature of equilibrium, the peak temperature and the hysteresis. The distribution incensement for the outcomes of alloys exhibits an increment in the range of temperature beyond 200^0C after the range $(100\text{-}170)^0$C and an increment in the loop of hysteresis, as illustrated in the Table 2. The distribution increment to the specimens S1 and S2 are noted in the Figure 11 and 12 for the DSC results of the SME DSC of these alloys. It's noticed that the test range exceeded the realized range (100-170^{0}C). That is owing to the influence of Tin addition that raised the limit of temperature of

the martensite. Such outcomes are corroborated via Saud et al. [8-9] and Abbass et al. [5-6] who inferred that the 4th element addition to shape memory material governs its characteristics. In Figure 13, there exist multi peaks as Sari [12] noted that these peaks are attributed to an interface transformation, and the two peaks are attributed with both phases (β`) and (γ`) of the transformation of martensite from β transfers to β`, which is a stabilized β, as depicted in the Figure 5.

Table 2: The results of the DSC test for the SMAs.

Alloy\Temperature(˚C)	A_s˚C	A_f˚C	M_s˚C	M_f˚C	T ˚C
Base	129	165	133	100	149
S1	150	183	122	92	153
S2	143	198	137	91	168
S3	206	225	128	88	177

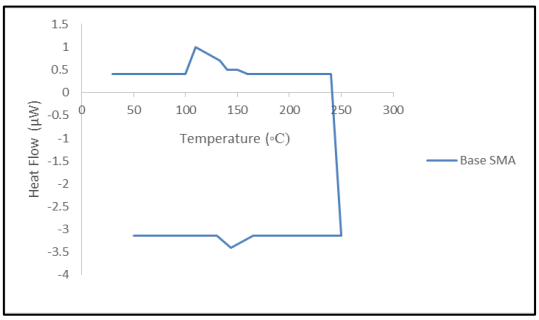

Figure 10: Thermogram of Base SMA.

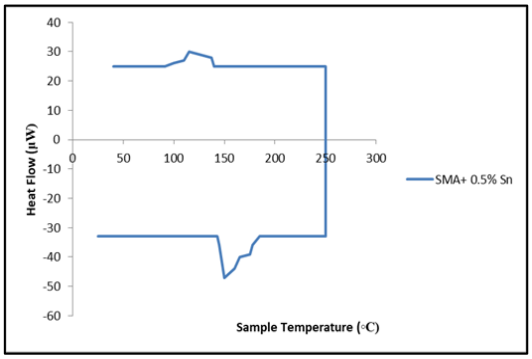

Figure 11: Thermogram of (S1) SMA.

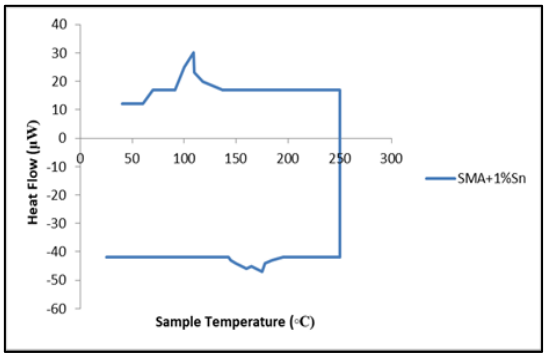

Figure 12: Thermogram of (S2) SMA.

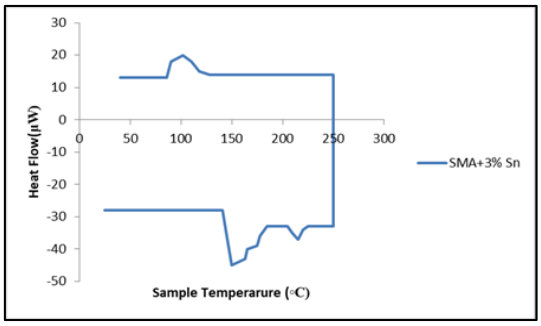

Figure 13: Thermogram of (S3) SMA.

IV. Mechanical Properties

Figure 14 shows the stress-strain diagram for base alloy and prepared SMAs, respectively whereas Table 3 lists the mechanical properties of the Alloys. It depicts an increment in the strain and the yield stress with the rise in Sn percentages, this behavior is owing to the fourth element addition to SMAs, as stated by Saud et al. [9] showed. It was found that the S3 alloy showed better results in the mechanical properties than S1 and S2 alloys. From the hardness results, it was noted that the HV of base alloy was slightly lower than the S1 alloy, and the S3 alloy revealed an increase over the limit, while the unbalanced phases did not affect the hardness. The increase in hardness with respect to the alloying elements was also observed by Abbass et al., in the addition of elements, like Te and Ge [6-7].,

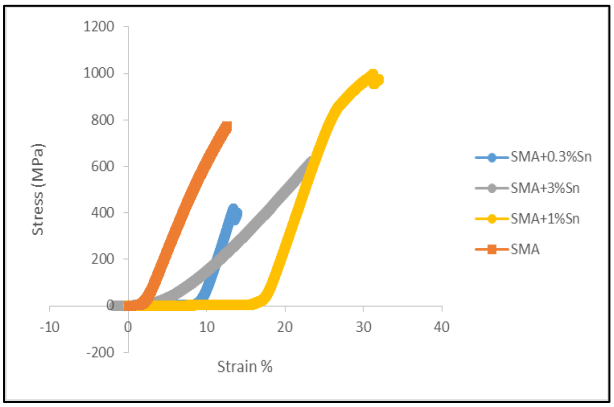

Figure 14: Stress – Strain Diagram.

As for the maximum stress, the S3 alloy showed the best result in stress and strain in similar manner that manifested by Saud et al. [9]. Compressive strength of the base SMA alloy (Cu-Al-Ni) provided the (S) changes shape with the addition of (Sn) [9], i.e. with raising the content of (Sn) to 1%. The strain and maximum compressive strength were from (13.5) to (32%) and (768) to (1200) MPa, respectively. These differences are due to the various volume fractions of the phase of (γ`) and/or the precipitates connected with the reduction of the density of porosity beyond the (Sn) addition. Generally, the precipitates size and volume fraction of precipitates possess a reverse influence on the mechanical properties of SMAs, as Saud et al. elucidated [9]. The greatest volume proportion of precipitates was obtained with addition of (3% Sn) that may cause the precipitates work like obstacles to the dislocation/phase interfaces motion, which causes the martensite transformation further difficult during the deformation process.

Table 3: Mechanical Properties of SMAs.

Alloy\Properties	HV	σ_y(MPa)	ε%	E (GPa)
Base	371	640	12.66	61.3
S1	391	358	13.53	21
S2	420	378	23.45	22.12
S3	530	846	31.97	50.07

V. Thermo-Mechanical Properties

Figure 15 evinces the stress-strain diagram for thermomechanical property of the base and prepared shape memory alloys at a stress (σ = 195 MPa), it's noticed that base SMA possesses higher strain recovery than the level of the prepared alloy below standard (3%) and attains to 1.07%, whereas the strain of the shape memory was from 0.64% to 0.35%. That is owing to the addition of (Sn) that improves greatly the mechanical properties with the raising of alloy, and these results are in agreement with those of Saud et al. [3], who deduced that the 4th elements influence the mechanical characteristics by controlling the mechanical processing.

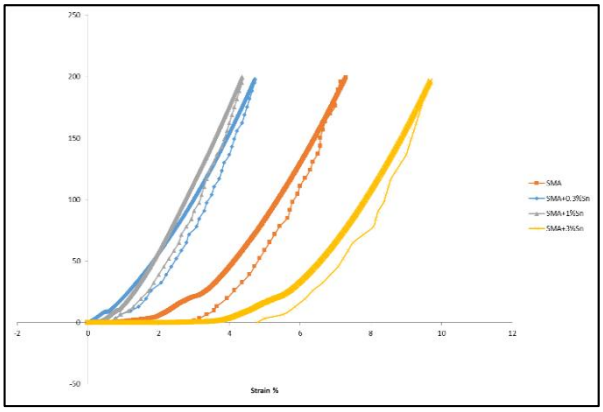

Figure 15: Thermo-Mechanical Stress –Strain Diagram.

The slope function available in EXCEL was used for computing the modulus of elasticity, as Lagudas [2] proposed from a computed data from Instron device. According to the Table 4, the modulus of elasticity of martensite is bigger than that for the austenite within the whole base alloy and the prepared alloys. That is owing to the twining which takes place at (σ = 135 MPa) [5] and the hardness of martensite is bigger than that of austenite, with an increment into the Sn quantity with acceptable error corresponding to Lagudas [2]

Table 4: Shape Memory Properties.

Alloy\Properties	ε%	Recovery%	E_M (MPa)	E_A (MPa)
Base	2.7	97.3	39.24	8.85
S1	0.64	99.3	100.5	78.95
S2	0.5	99.5	106.2	90.99
S3	4%	95%	58.59	44.84

4. Conclusions

1. The microstructure showed both shapes of Martensite the stack pile (γ`) and the Needle shape (β`) also microstructure showed in the S2 and S3 alloys.
2. It was found that Tin addition to the Shape Memory Alloy has raised the transformation temperatures, and in the case of S3 alloy the rise was beyond the domain.
3. Sn addition also improved Mechanical properties of the Shape Memory Alloy raised the Yield Stress. Tin Addition gave improvement in shape memory properties and S2 Alloy gave the best results.

Acknowledgement

The author acknowledges the staff of the X-Ray Diffraction Unit in Nano Technology and Advance Materials Center at University of Technology-Baghdad-Iraq, staff of Heat Transfer Lab and the Strength of Materials Lab in the Department of Materials Engineering/University of Technology, and staff of SEM EDS Lab in the Department of Production Engineering and Metallurgy at University of Technology-Baghdad-Iraq.

References

[1] C. L'excellent, "Shape Memory Alloy Handbook "John Wiley and Son, 2nd ed., New York, USA, 2013.

[2] D. Lagudas, "Shape Memory Alloy: Engineering Modeling" Springer, end ed., Berlin, Germany, 2010.

[3] J. W. Kim, D. W. Ro, E. S. Lee, and Y. G. Kim, " Effects on Microstructure and Tensile Properties of a Zirconium Addition to a Cu-AI-Ni Shape Memory Alloy", Metallurgical transaction A, Vol.21A, No.11, pp.741-744, 1990.

[4] J. M. Jani , M. Leary, and A. Sibic, "A review of Shape memory alloy research applications and opportunities", Materials and Design, Vol. 6, No. 3, pp.1078-1133, 2014.

[5] J. Van Humbeeck, "Non-medical application of shape memory alloys", Material Science and Engineering, Vol. 273, No. 275, pp. 134-148, 1999.

[6] M. K. Abbass, M. M. Rahdi, and R. S. A. Adnan, "The effect of Germanium Addition on mechanical Properties and microstructure of Cu-Al-Ni Shape Memory Alloy", Materials Today: Proceedings, Vol. 4, No. 10, pp. 224–233, 2017.

[7] M. K. Abbass, M. M. Rahdi, and R. S. Ahmed Adnan, "The effect of Tellurium Addition on mechanical Properties and microstructure of Cu-Al-Ni Shape Memory Alloy", International Journal of Advances in Science, Engineering and Technology (IJASEAT), 4, 2, pp. 161-164, 2016.

[8] S. N. Saud, E. Hamzah, T. Abubakar, and R. S. Hosseinian, "A Review on Influence of Alloying Elements on the Microstructure and Mechanical Properties of Cu-Al-Ni Shape Memory Alloys", Journal Technology (Sciences & Engineering), Vol.b64, No. 1, pp. 51–56، 2013.

[9] S. N. Saud, E. Hamzaha. T. Abubakar, M. Ibrahim K., and Bahador Abdullah, "Effect of a fourth alloying element on the microstructure and mechanical properties of Cu–Al–Ni shape memory alloys", Journal of Materials,Vol. 30, No. 14, pp. 2285-2269, 2015.

[10] R. S. Ahmed Adnan and M. M. Abudlbaki, "Effect of Sn Addition on Transformation Temperature and Thermal Properties for Cu-Al-Si Shape Memory Alloy", IOP Conf. Ser.: Mater. Sci. Eng. 454, 1, 012050, 2018.

[11] G. A. L´opez, M. Barrado, J. M. San Juan, and M. L. N´o, "Interaction of Cu–Al–Ni shape memory alloys particles with molten In and In + Sn matrices", Materials Science and Engineering A, Vol. 495, No. 1 , pp. 304–309, 2008.

[12] U. Sari, "Influences of 2.5wt.% Mn addition on the microstructure and mechanical properties of Cu-Al-Ni shape memory alloys", International Journal of Minerals, No.17, pp. 2-14, 2010.